

Special Session: When Dataflows Converge: Reconfigurable and Approximate Computing for Emerging Neural Networks

Di Wu and Joshua San Miguel

Department of Electrical and Computer Engineering, University of Wisconsin–Madison, Madison, Wisconsin, USA
di.wu@ece.wisc.edu, jsanmiguel@wisc.edu

Abstract—Deep Neural Networks (DNNs) have gained significant attention in both academia and industry due to the superior application-level accuracy. As DNNs rely on compute- or memory-intensive general matrix multiply (GEMM) operations, approximate computing has been widely explored across the computing stack to mitigate the hardware overheads. However, better-performing DNNs are emerging with growing complexity in their use of nonlinear operations, which incurs even more hardware cost. In this work, we address this challenge by proposing a reconfigurable systolic array to execute both GEMM and nonlinear operations via approximation with distinguished dataflows. Experiments demonstrate that such converging of dataflows significantly saves the hardware cost of emerging DNN inference.

I. INTRODUCTION

Research into deep neural networks (DNNs) has been prospering in both academia and industry since the championship of convolutional neural networks (CNNs) in image recognition [5], with broad applications in computer vision, natural language processing, speech recognition, etc. DNN models are intensive in general matrix multiply (GEMM) operations [2], e.g., more than 90% of total operations are GEMM. To mitigate the overhead in executing GEMMs, significant efforts have been paid to approximate computing, including approximate multipliers, either fixed units at design-time or reconfigurable units at run-time, and the high level synthesis of those approximate multipliers [13]. Those techniques reduce both the energy and power consumption for GEMMs at the cost of insignificant accuracy loss.

However, emerging DNNs with more sophisticated nonlinear operations are benefiting less than classical DNNs, like CNNs, from those approximation techniques, as more sophisticated nonlinear operations than ReLU or max pooling [7] can mitigate or even diminish the energy and power improvements. Those nonlinear operations, e.g., *div*, *exp*, *log*, *tanh*, *sigmoid*, *softmax*, etc., are of high complexity, high diversity and high cost [12]. Naively implementing those nonlinear operations alongside the approximate multipliers can increase the area and power to nearly 6.0× and 4.2×, respectively [12]. To address such inefficiencies, in [12] we initially propose to leverage existing multiply-accumulate (MAC) units to virtualize those nonlinear operations in a unified manner, so that the hardware overhead to execute those nonlinear operations can be minimized. We extend a standard MAC unit with extra logic,

including least zero detection, shifters, lookup tables (LUTs), adders and multiplexers (MUX), to extensively support diverse nonlinear operations. Despite improved compatibility, those add-ons slatted on a single processing element (PE) still introduce high overheads, costing more area and power than an individual MAC unit.

In this paper, to further mitigate the above area and power overheads, we propose to *virtualize the nonlinear operations on eagerly optimized dataflow architectures*. More specifically, we equip systolic arrays with the additional capability to approximate nonlinear operations. The proposed design is highlighted with three features compared with [12]. First, *the dataflows for GEMM and approximate nonlinear operations converge inside one single architecture*. A weight stationary dataflow is applied in Google TPU [3], a commercialized systolic array for DNNs. We also observe that another weight stationary dataflow can be applied to the Taylor approximations with Horner’s rule [12]. As such, we merge the two weight stationary dataflows inside one architecture. Second, *our design disperses the extra logic in multiple PEs to increase the architectural-level area and power savings*. Though the dataflows for GEMM and Taylor approximations are both weight stationary, their PE designs differ. In [12], each PE is extended with all required add-ons and able to perform a complete operation. In the dataflow architecture, each PE only performs a certain part of an operation. Our systolic array removes unnecessary parts in each PE to save more compared to arrays with all holistic PEs. Third, *our design involves an architectural-level approximation, orthogonal to existing microarchitecture-level approximation techniques*. Our design targets the architecture-level approximation of varying operations, i.e., we define the interaction among different PEs, beyond the microarchitecture-level approximations as in [1, 4, 9, 12, 13]. Such a different viewpoint allows the coexistence of both the architecture- and microarchitecture-level optimizations for further savings.

We list the contributions in this work as follows.

- We identify the deficiency of existing works in approximating nonlinear operations as the dedication to a single PE, raising the cost of the entire PE array.
- We propose a cross-level approximated systolic array to incorporate both GEMM and nonlinear operations and amortize the area and power overheads across multiple

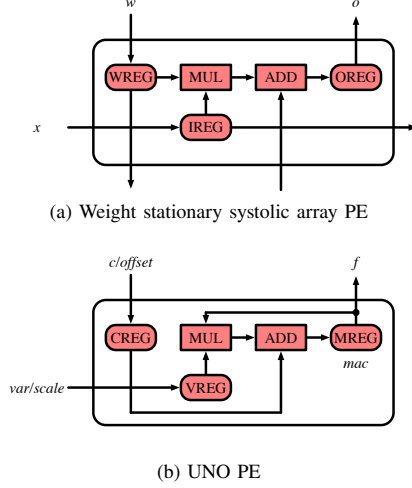


Fig. 1: PEs for GEMM and UNO dataflows. XREG refers to data registers, while MUL and ADD refer to the multiplier and adder.

PEs for excessive hardware savings.

- We evaluate the accuracy and hardware efficiency of our design on emerging DNNs with complex nonlinear operations, demonstrating its superior area, power and energy benefits over existing designs.

The rest content is organized as follows. Section II reviews the weight stationary systolic array [3] and unified nonlinear operations [12]. Then Section III articulates our proposal, which is later evaluated in Section IV. The final Section V concludes the paper.

II. BACKGROUND

A. Weight Stationary Systolic Array

The weight stationary dataflow for GEMM, i.e., $o = x \cdot w$, is applied in systolic arrays like Google TPU [3], which contains multiple rows and columns of the PE in Figure 1a. First, the weight w is loaded into the weight register, i.e., WREG. Multiple cycles are needed to load a weight to the correct PE from top to bottom. Second, the input x is continuously streamed into the input register, i.e., IREG, and pipelined to the right PE in the next cycle. Finally, the output o is calculated by summing the partial result from the bottom PE and the product of the weight and input in the current PE. When all outputs corresponding to the current weights are streamed out, the above three steps are repeated for a complete GEMM operation. For the weight stationary dataflow, there have been a plethora of schedule algorithms, some of which are publicly available [8, 11].

B. Unified Nonlinear Operation

In [12], we propose to unify multiple nonlinear operations (UNO), e.g., y/x , $\exp(x)$ and $\log(x)$, using Taylor approximation for minimized hardware overheads. Taylor approximation in Equation 1 is formulated as in Equation 2 and Equation 3

using Horner's rule. In Equation 1, $f^{(i)}(a)$ is the i -th derivative of f evaluated at input $x = a$, and c_i denotes the coefficient of the i -th term. Then in Equation 2 and Equation 3, mac_n is the cascaded MAC result for degree- n Taylor approximation, $scale$ and $offset$ are used to adjust mac_n to the correct result, and var is an affine transformation of input. Equation 3 requires var $0 \leq x \leq 1$ for \exp and $0.5 \leq x \leq 1$ for \log . Please refer to [12] for calculating $scale$, $offset$ and var in detail.

$$f_n(x) = \sum_{i=0}^n \frac{f^{(i)}(a)}{i!} \cdot (x-a)^i = \sum_{i=0}^n c_i \cdot (x-a)^i, \quad (1)$$

$$f_n(x) = offset + mac_n \cdot scale, \quad (2)$$

$$mac_i = \begin{cases} |c_{n-i}| + mac_{i-1} \cdot var & \text{if } 1 < i \leq n, \\ |c_{n-1}| + |c_n| \cdot var & \text{if } i = 1, \end{cases} \quad (3)$$

As such, every step in UNO is a MAC operation, whose PE is shown in Figure 1b. Note the logic for the coefficients c , $scale$, $offset$ and var are not shown for simplicity. $scale$, $offset$ and var are input dependent, requiring extra hardware. In [12], the choice of building a SIMD architecture based on UNO leads to the duplication of those extra hardware in every PE, throttling the overall area and power savings.

In this work, by observing that the coefficients c are independent from the input, and can be statically stored, leading to a weight stationary dataflow, we propose to merge the two PEs in Figure 1 to a reconfigurable one, minimizing the overheads to support multiple dataflows at the architecture level.

III. THE PROPOSED DESIGN

A. Processing Element

The proposed PEs towards the convergence of GEMM and UNO dataflows are presented in Figure 2. The red components are identical to those in Figure 1a, serving the original GEMM dataflow. Unlike the PE in Figure 1a, our PEs are heterogeneous with different inputs and outputs. Then the blue components are added to route the data path to act as in Figure 1b, serving the UNO dataflow. But unlike the UNO PE in Figure 1b, the proposed PEs do not calculate the complete output in an individual PE, but rather circulate an intermediate result to the right PE, i.e., the approximation is now performed spatially instead of temporally. The double stroke means both x in IREG and var in VREG are pipelined to the right PE. The VREG is present together with IREG to minimize the overall area and power; otherwise, the more expensive var logic needs to exist in all PEs to generate var , $scale$ or $offset$. For example, var is needed when $1 \leq i \leq n$ in Equation 3. For area and power saving, its calculation is done only in the leftmost PE, with its value pipelined to right PEs. Then $scale$ and $offset$ are accessed at the last step, so their logic can exist merely in the rightmost PE (or a few rightmost PEs with proper pipelining to ensure a reasonable critical path overhead, not shown in the figure). Note that y in the rightmost PE is only used in y/x , not in $\exp(x)$ and $\log(x)$.

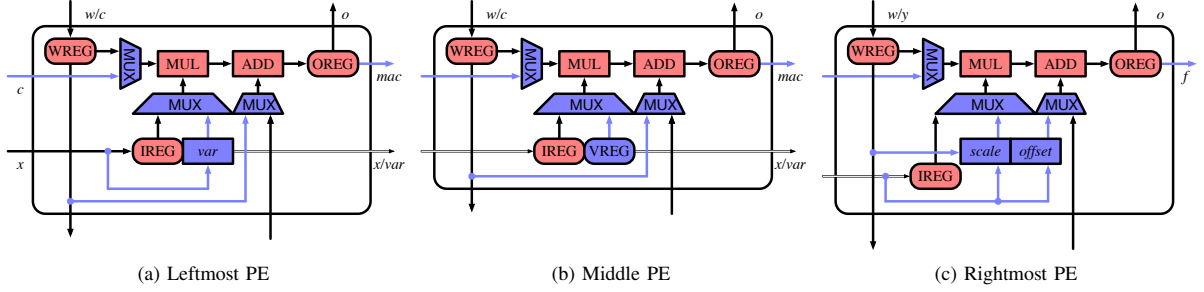


Fig. 2: The proposed PEs for hybrid dataflows. Corresponding PEs are located at the leftmost, middle and rightmost columns. The red and blue colors are for GEMM and UNO dataflows, respectively.

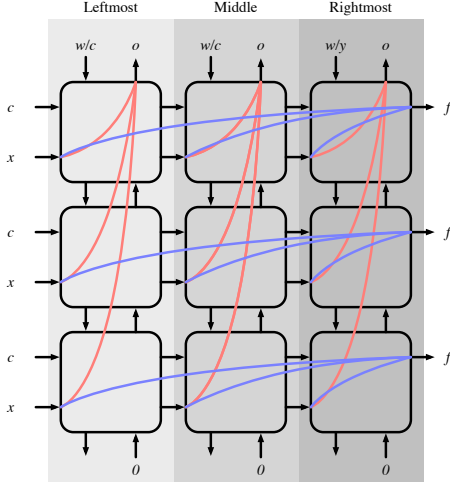


Fig. 3: The proposed systolic array for hybrid dataflows. The red and blue colors are for GEMM and UNO dataflows, respectively.

B. Systolic Array

With above heterogeneous PEs, we further present the entire systolic array as in Figure 3, which contains one column of leftmost, middle and rightmost PEs. We mark the essential inputs and outputs surrounding the systolic array, and emphasize the GEMM and UNO dataflows, i.e., how the input x flows in the systolic array to produce the output o and f . In both dataflows, the input x are pipelined from left to right PEs. The GEMM dataflow in red aggregates the partial results vertically, from bottom to top, in each column. The input x , weight w and output o are all stored in the on-chip SRAM, which needs to interact with the off-chip DRAM [3]. On the other hand, the UNO dataflow in blue collects the partial results horizontally, from left to right, in each row. The input x and output o also need to travel inside the memory hierarchy, including both the SRAM and DRAM. However, the coefficients c are stored with small LUTs, as they are predetermined and remain identical in each column. For example, to support *div*, *exp* and *log* simultaneously, 2 and 1 3-entry LUTs are needed for c

in the leftmost and middle columns, respectively. Given the size of the systolic array as R -row-by- C -column, one set of *var*, *scale* and *offset* logic is shared by one row of C PEs, instead of per PE in [12], effectively reducing the area and power overheads. In terms of dataflow schedule, we only need to address the newly introduced UNO dataflow. Its schedule is even simpler than the GEMM dataflow, as it is purely elementwise, requiring minimal effort. Such an elementwise behavior nearly reduces the memory access conflicts to zero.

C. Cross-Level Approximation

The above systolic array approximates nonlinear operations at the architecture level. Applying more eager microarchitecture-level approximations [1, 4, 9] leads to a cross-level approximation to further reduce the area and power. We look at a simple *heuristic* approximation, instead of the accuracy-guaranteed approximation [6, 9]. Observing that UNO dataflow proceeds from high to low order, the lower-order Taylor terms are multiplied fewer times and can be more eagerly approximated. Thus, we can apply less bits to the PEs on the right, e.g., each PE has one less fraction bit than its left PE. For example, a N -bit design of size R -by- C has N -bit inputs for MAC in the leftmost PE, and $(N - C + 1)$ -bit inputs for MAC in the rightmost PE.

IV. EVALUATION

A. Experimental Setup

This work aims to improve the efficiency of emerging DNNs with 1) a PE-enhanced systolic array and 2) a cross-level approximation, therefore both accuracy and performance are evaluated. The accuracy is simulated with customized PyTorch operators [10], covering both the operation- and application-level results. Note that no retraining is involved to minimize accuracy loss. The evaluated DNN is the CapsNet model in [12], containing *div*, *exp*, *log*, *sigmoid* and *softmax*. On the other hand, the performance evaluation, in terms of area, power and energy efficiency, is done with 32nm TSMC technology under 400MHz. We set the array size of our design and the SIMD UNO array (of size $R \cdot C$) to $R = C = 4$ and $R = C = 8$ and bit width to $N = 16$.

B. Accuracy

1) Operation-Level

The operation-level absolute root mean square error of our design is presented in Table I (Other values can be obtained using the *scale* logic without accuracy drop). We observe that our design exhibits slightly higher error compared to UNO with an identical cycle C . Moreover, with a longer cycle count C , our design incurs higher errors due to less-bit MACs at the end, in contrast to UNO’s increasing accuracy.

TABLE I: Absolute root mean square error of nonlinear operations with certain input ranges. The total 16 bits are assigned as 1-bit sign, 5-bit integer and 10-bit fraction.

Operation (Input range)	Ours (R, C, N)		UNO (R, C, N)	
	4,4,16	8,8,16	4,4,16	8,8,16
<i>div</i> ($y = 1, 0.5 \leq x \leq 1$)	0.022	0.039	0.021	0.001
<i>exp</i> ($0 \leq x \leq 1$)	0.080	0.032	0.079	0.001
<i>log</i> ($0.5 \leq x \leq 1$)	0.005	0.026	0.005	0.000

2) Application-Level

The DNN accuracy is shown in Table II. The floating-point model has an accuracy of 98.78%. Our design has similar accuracy loss compared to C -cycle UNO, even with the cross-level approximation in most cases. For $R = C = 8$ and $N = 16$, our design has an obvious accuracy drop due to the cross-layer approximation aggressively reduces the fraction bits.

TABLE II: Accuracy of CapsNet inference with varying allocations of the 16 bits to the sign, integer and fraction.

Sign-Integer-Fraction (bit)	Ours (R, C, N)		UNO (R, C, N)	
	4,4,16	8,8,16	4,4,16	8,8,16
1-7-8	98.70	86.27	98.69	98.68
1-6-9	98.87	97.75	98.87	98.85
1-5-10	98.75	98.36	98.76	98.78
1-4-11	94.05	93.55	93.98	93.78

C. Performance

The performance results are in Table III, with a focus on the computing kernel. The total 16 bits are allocated as 1-bit sign, 5-bit integer and 10-bit fraction.

TABLE III: Hardware efficiency of the computing kernel.

Performance	Ours (R, C, N)		UNO (R, C, N)		Improve (%)	
	4,4,16	8,8,16	4,4,16	8,8,16	4,4,16	8,8,16
Area (mm ²)	0.13	0.41	0.18	0.73	29.4	43.3
Power (mW)	8.33	28.52	11.45	46.12	27.2	38.2
Throughput (ksamples/s)	0.15	0.52	0.15	0.52	0.0	0.0
Energy Efficiency (ksamples/J)	18.58	18.34	13.52	11.34	37.4	61.7

1) Area

The overall area of our design is up to 43.3% smaller than UNO, due to three reasons. First, the extra logic to support nonlinear operations is shared by multiple PEs in our design, amortizing the overhead over MAC units. The overhead is reduced from 38.9% in UNO to 15.7% in our PEs. Second, our design allows a cross-level approximation without significant

accuracy loss. The cross-level approximation reduces the area by 27.8% compare to an array without the extra microarchitectural approximation. Third, our design is a systolic array, which accumulates inside the array, while UNO requires an additional adder tree for accumulation. The adder tree contributes to around 7% of the total UNO area.

2) Power

The power results of our design and UNO are shown in Table III. Our design also exhibits smaller power, up to 38.2%, due to identical reasons in the area.

3) Energy Efficiency

To achieve the energy efficiency, we first estimate the throughput (the reciprocal of runtime) of CapsNet for our design and UNO. Data schedule for perfect runtime is beyond the scope of this work. Instead, we assume that the computing arrays in our design and UNO both have a utilization of 50% for GEMM and 80% for nonlinear operations to estimate the runtime, which is identical to that in [12]. Then the energy efficiency is computed as the throughput divided by the power. Due to the smaller power, our design outperforms UNO in terms of the energy efficiency by up to 61.7%.

V. CONCLUSION

In this work, we identify the overheads of our initial work in executing nonlinearity-intensive emerging deep neural networks. We propose a reconfigurable systolic array to flexibly execute the dataflow for either GEMM or nonlinear operations and boost the efficiency with the cross-level approximation, including both the architecture and microarchitecture levels. The area, power and energy efficiency of our design is up to 43.3%, 38.2% and 61.7% higher than our initial work. The accuracy simulation codes are available online [10].

REFERENCES

- [1] S. Behroozi *et al.*, “SAADI: A scalable accuracy approximate divider for dynamic energy-quality scaling,” in *ASPDAC*, 2019.
- [2] Y. Jia, “Learning semantic image representations at a large scale,” Ph.D. dissertation, UC Berkeley, 2014.
- [3] N. P. Jouppi *et al.*, “In-datacenter performance analysis of a tensor processing unit,” in *ISCA*, 2017.
- [4] T. Kemp *et al.*, “MIPAC: Dynamic input-aware accuracy control for dynamic auto-tuning of iterative approximate computing,” in *ASPDAC*, 2021.
- [5] A. Krizhevsky *et al.*, “Imagenet classification with deep convolutional neural networks,” in *NeurIPS*, 2012.
- [6] S. Lee *et al.*, “High-level synthesis of approximate hardware under joint precision and voltage scaling,” in *DATE*, 2017.
- [7] V. Nair and G. E. Hinton, “Rectified linear units improve restricted Boltzmann machines,” in *ICML*, 2010.
- [8] A. Samajdar *et al.*, “SCALE-Sim: Systolic CNN accelerator simulator,” *arXiv*, 2018.
- [9] D. Wu *et al.*, “SECO: A scalable accuracy approximate exponential function via cross-layer optimization,” in *ISLPED*, 2019.
- [10] D. Wu, “RAVEN.” [Online]. Available: <https://github.com/diwu1990/RAVEN>
- [11] D. Wu, “uSystolic-Sim.” [Online]. Available: <https://github.com/diwu1990/uSystolic-Sim>
- [12] D. Wu *et al.*, “UNO: Virtualizing and unifying nonlinear operations for emerging neural networks,” in *ISLPED*, 2021.
- [13] G. Zervakis *et al.*, “Approximate computing for ML: State-of-the-art, challenges and visions,” in *ASPDAC*, 2021.